A Physics-Informed Variational Autoencoder for Rapid Galaxy Inference and Anomaly Detection

Anonymous Author(s)
Affiliation
Address
email

Abstract

The Vera C. Rubin Observatory is slated to observe nearly 20 billion galaxies during its decade-long Legacy Survey of Space and Time. The rich imaging data it collects will be an invaluable resource for probing galaxy evolution across cosmic time, characterizing the host galaxies of transient phenomena, and identifying novel populations of anomalous systems. To facilitate these studies, we introduce a convolutional variational autoencoder trained to rapidly estimate the redshift, stellar mass, and star-formation rate of galaxies from multi-band imaging data. We show that our CVAE can be used to identify physically-meaningful anomalies in large galaxy samples >100x faster than the leading parameter inference techniques.

1 Introduction

At the cornerstone of a range of diverse astrophysical domains sits the chemical and dynamical histories of galaxies. Aspects of these histories can be inferred piecewise from observations. From broad-band photometry, one can infer the underlying spectral energy distribution (SED); using morphological features, one can reconstruct a galaxy's merger/interaction history. Novel galaxy sub-populations have been discovered through detailed manual inspection along these axes; some prominent examples include 'Green Pea galaxies', defined by their compact shapes and high star-formation rates [6]; and 'passive Red Spirals'– spiral galaxies with minimal star formation, whose colors seem to contradict a morphology that is commonly tied to much more active galaxies [13].

The rise of deep convolutional neural networks, which allow for morphological classification of galaxies from image data [7], and of simulation-based inference to estimate their underlying SED parameters from photometry [17], have paved the way for low-latency galaxy analysis in the era of synoptic surveys. However, anomaly detection within these frameworks remains an open question: out-of-distribution events may be identified by flagging high reconstruction errors at test time [e.g., 16], but this approach can produce samples contaminated by non-astrophysical anomalies such as poorly-calibrated images and chip gaps.

Here, we introduce a technique to guide the latent features of a convolutional variational auto-encoder (CVAE) toward the physical parameters of a galaxy. CVAEs are a class of neural network designed for compression. Variational AEs, in particular, typically employ the Kullback–Leibler (KL) divergence to enforce a continuous and probabilistic latent distribution characterized by a multivariate standard Normal. CVAEs have been extensively used in the literature for galaxy image reconstruction [14, 8, 3]. Here, we extend this methodology to disentangle the observational properties of a galaxy (e.g., its orientation) from its intrinsic properties in the latent space, and discover more meaningful anomalies.

Submitted to 37th Conference on Neural Information Processing Systems (NeurIPS 2023). Do not distribute.

2 Data and Methodology

In this section, we describe our methodology for designing and training a physics-informed CVAE. Our CVAE encodes a galaxy image into 5 latent dimensions, the first four corresponding to the orientation, redshift, stellar mass, and star-formation rate of the galaxy. The fifth dimension encodes any remaining structure not captured by the first four features.

We select a sample of $z < 1$ spectroscopic galaxies from both the LSST deep drilling fields catalogue from [18] (hereafter, the Z22 sample) and from GAMA DR4 [9]. These catalogues report the average star-formation rate and stellar mass of each galaxy obtained with the SED-fitting codes `CIGALE` and `PROSPECT`, respectively, along with their associated uncertainties. We include the Z22 sample to provide training support at high redshift, and the GAMA catalogue to includes low-redshift objects for which rich morphological information is available. For galaxies that overlap with the Dark Energy Camera Legacy Survey (DECaLS) footprint, we then download 128x128 px DECaLS co-added images centered at the location of each galaxy in grz[1]. DECaLS data reaches a 5-σ depth of $g \sim$24, making it a sufficient analog for upcoming Rubin data ($g \sim$24.5[2]). We remove five galaxies that are missing images in at least one filter, leaving us with a combined sample of 26,126 galaxies.

We pre-process our images in each filter b by applying the following normalization [2]:

$$x_b = \tanh\left(\sinh^{-1}\left(\beta \frac{\mathrm{x_{raw,b}}}{\langle \max(\mathrm{x_{raw,b}})\rangle_{\mathrm{b}}}\right)\right) \tag{1}$$

where $\beta = 10$. We then interpolate each image to 69x69 px to reduce training times.

Next, we use the `photutils` package to estimate the orientation of each galaxy. We stack the grz images and subtract the median background level from the stack, assuming a 10x10 px box size and a 3x3 px median filter. We then convolve each background-subtracted image with a 2d Gaussian filter and construct a catalog of all identified sources. The morphological features of each source are calculated by default, and we extract the orientation of the source with centroid closest to the center of the image. We then split our data into an 80% training sample and a 20% validation sample.

To assess the utility of our CVAE for anomaly detection, we augment our validation set with a sample of 294 Red Spiral galaxies from [13] and the KISS sample of 13 Green Pea galaxies [5]. The Red Spiral galaxies were consolidated by the 160,000 volunteers of the Galaxy Zoo project.

We construct our CVAE using the same architecture as in [1][3]. The network consists of three convolution encoding layers, three deconvolution decoding layers, and a latent dimension of 5. We train the network using a loss function consisting of three terms. The first is the reconstruction loss, the second is the KL divergence between the fifth latent feature and a standard Normal, and the third is the mean squared error between the first four latent features and the galaxy's physical properties:

$$L = \beta_0 \frac{1}{n}\sum_{i=1}^{n}(x_i - \hat{x_i})^2 + (\sigma_5^2 + \mu_5^2 - log(\sigma_5) - 1) + \beta_1 \frac{1}{n}\sum_{i=1}^{n}\frac{1}{\sigma_p^2}(p - \mu)^2 \tag{2}$$

where p is a vector containing the physical properties of the galaxy (orientation, spectroscopic redshift, and survey-reported stellar mass and star-formation rate) and σ_p are their reported uncertainties (we assume an uncertainty of 0.1 rad for all calculated orientations). The coefficients β_0 and β_1 are hyperparameters; we have found through moderate tuning that setting $\beta_0 = 10$ and $\beta_1 = 50$ results in reasonable parameter estimates without significantly degrading the quality of reconstructed images.

As a baseline comparison, we train a vanilla CVAE with the same architecture but excluding the physical term from the loss function (the KL-divergence is now calculated across all 5 latent features, which are unphysical). We train each network for 1000 epochs using the standard Adam optimizer [12] with a learning rate of 5×10^{-6} and a batch size of 128 on two GPUs, confirming convergence of the loss, and save the model weights at the epoch where the validation loss is minimized. Our code and trained models can be found at the associated github repository for this work[4].

[1] `https://www.legacysurvey.org/decamls/`

[2] `https://www.lsst.org/scientists/keynumbers`

[3] `https://github.com/jwuphysics/galaxy-autoencoders.`

[4] Redacted.

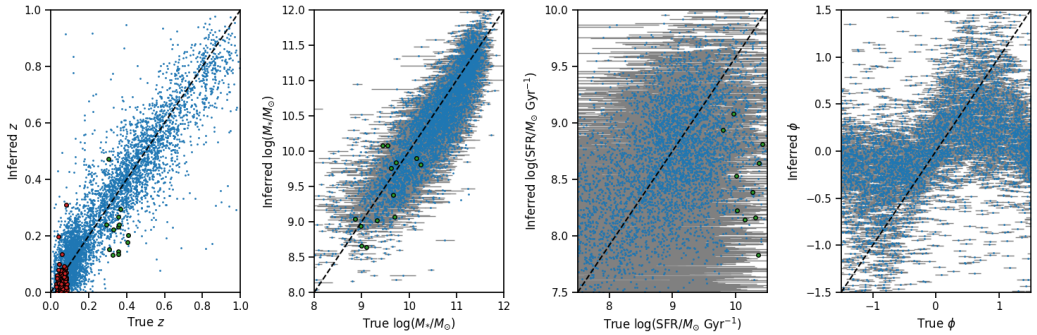

Figure 1: A comparison between the learned latent features of the CVAE applied to the validation set, and the physical properties of the associated galaxies derived through SED fitting. 1-σ uncertainties on SED-estimated parameters are shown in gray. Literature values for Green Pea galaxies are given in green, and those for Red Spirals are given in red (only redshift is reported for Red Spirals).

3 Results and Discussion

The catalog-level and CVAE-estimated physical properties for the validation sample are compared in Fig. 3. The CVAE is largely able to infer the physical parameters of galaxies in the validation set; the predictions appear unbiased and few catastrophic outliers are observed (the scatter is large for star-formation rate, but comparable to the error bars on reported SED estimates). An exception is the orientation ϕ: because the parameter is periodic in nature (galaxies with orientations $\pi/2$ and $-\pi/2$ are indistinguishable), this feature is poorly reconstructed at the extremes. We evaluate the performance of our CVAE at redshift estimation using a similar set of metrics as other photometric redshift methods [10]. We calculate a mean squared error of 0.01, a bias of 0.001, a mean absolute deviation (MAD) of 0.05, and an outlier fraction of 0.1 (where we have defined an outlier as deviating $> 15\%$ from the spectroscopic measurement). Our MAD is higher than that reported by [4] (0.02), who use a training set of 3M galaxies (150x larger than our sample); our bias is comparable.

Surprisingly, our network is able to predict reasonable estimates for the spectroscopic redshifts and stellar masses of the anomalous galaxies from images alone, despite the anomalous colors of the Red Spiral and Green Pea galaxies. The redshifts of the Green Peas are still systematically underestimated, which skews the predicted star-formation rates downward.

We construct a simple support vector machine (SVM) classifier to identify our anomalous galaxies using only encoded features. We use the implementation from `scikit-learn`, with a radial basis function kernel and default parameters. After over-sampling with `SMOTE` to balance our classes, our trained classifier recovers 100% of Green Pea galaxies with a 2% contamination rate from non-anomalous galaxies, and 98% of Red Spiral galaxies with a 5% contamination rate.

We plot 2d projections of the latent space for the physics-informed and baseline CVAE models in Fig. 3. For the physics-informed plots, we include the decision boundaries from a 2d SVM with linear kernel. Though the Red Spirals fall toward the edges of the latent parameter distributions in the baseline, the plots lack physical intuition. The latent space of the physics-informed CVAE, however, reveals the properties that make these sub-populations anomalous. Green Pea galaxies push toward the highest star-formation rates, lowest stellar masses, and lowest "morphology" values of the sample (this can be considered a proxy for compactness). Red Spirals, in contrast, are the most extended objects in the sample and have low star-formation rates for their stellar masses, with most falling in or below the 'green valley' that distinguishes active from quenched galaxies [15].

Finally, we identify galaxies in our sample most similar to the labeled Green Peas and Red Spirals. We use the `NearestNeighbor` method in `scikit-learn` to identify ten galaxies in the non-anomalous sample with latent features most similar to each galaxy in the anomalous sample. We present a sample of galaxies with lowest latent-space Minkowski distance to multiple Red Spirals, and those with lowest distance to multiple Green Peas, in Fig. 3. These galaxies are prime targets for upcoming follow-up studies, to confirm their associations and further characterize their evolutionary histories.

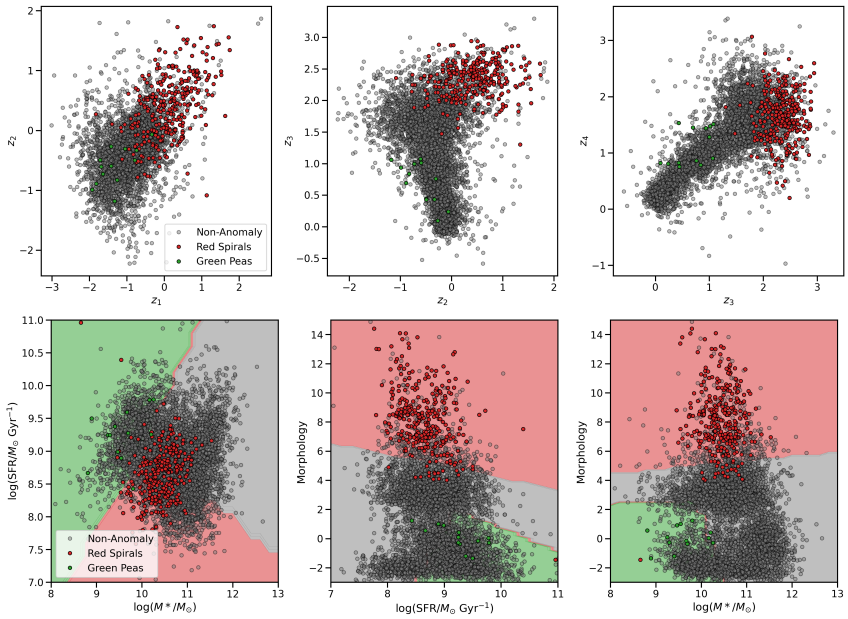

Figure 2: Projections of the latent features drawn for the validation set, including the two populations of anomalies. Sub-types are given in legend. **Top row:** Latent space for the vanilla CVAE, trained without physics-informed loss constraints. **Bottom Row:** Latent space for our physics-informed CVAE, with two-dimensional SVM decision boundaries overplotted. Green Peas are identified by their compact morphologies, low stellar masses, and high star-formation rates; Red Spirals are identified by their extended morphologies, higher stellar masses, and lower star-formation rates.

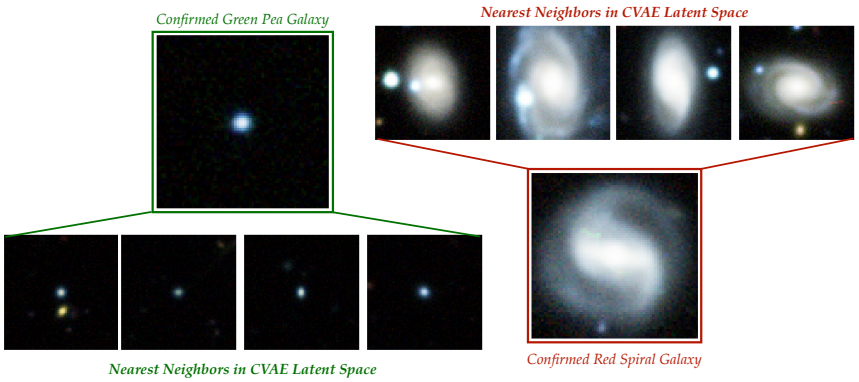

Figure 3: Latent space nearest-neighbors for the anomalies manually flagged in the Galaxy Zoo project. **Left:** Images of galaxies with latent properties most similar to labeled "Green Pea" galaxies. **Right:** Images of galaxies most similar to labeled "Red Spiral" galaxies. These galaxies are less blue than the majority of other spirals in our sample, suggesting older average stellar populations.

The ability to rapidly infer physical parameters competitive with state-of-the-art SED models using only three images of a galaxy is encouraging. Once trained, evaluation of our CVAE takes 7 ms per galaxy on an Apple M2 Max chip. This is substantially less than the $\sim$10 hrs required for rigorous SED fitting using modern approaches [11], and $>$ 100x faster than existing simulation-based inference (SBI) models optimized for this task [17]. With our approach, estimating the redshift, stellar mass, and star-formation rate of all 20B galaxies observed by the Vera C. Rubin Observatory would require only $\sim$1500 CPU-hours (albeit without the added benefit of full posterior distributions, as are provided by SBI). New, neural network-based inference approaches like the one presented here will help bring scalability and interpretability to petabyte-scale data exploration among astronomical surveys, and facilitate the search for new galaxy sub-types.

References

[1] What do galaxies look like? learning from variational autoencoders. `https://jwuphysics.substack.com/p/galaxy-autoencoders`. Accessed: 2023-09-29.

[2] B. Arcelin, C. Doux, E. Aubourg, C. Roucelle, and LSST Dark Energy Science Collaboration. Deblending galaxies with variational autoencoders: A joint multiband, multi-instrument approach. , 500(1):531–547, Jan. 2021. doi: 10.1093/mnras/staa3062.

[3] B. Arcelin, C. Doux, E. Aubourg, C. Roucelle, and LSST Dark Energy Science Collaboration. Deblending galaxies with variational autoencoders: A joint multiband, multi-instrument approach. , 500(1):531–547, Jan. 2021. doi: 10.1093/mnras/staa3062.

[4] R. Beck, I. Szapudi, H. Flewelling, C. Holmberg, E. Magnier, and K. C. Chambers. PS1-STRM: neural network source classification and photometric redshift catalogue for PS1 3π DR1. , 500(2):1633–1644, Jan. 2021. doi: 10.1093/mnras/staa2587.

[5] S. W. Brunker, J. J. Salzer, B. Kimsey-Miller, and B. Cousins. The Environments of Green Pea Galaxies. I. The KISS Sample. , 926(2):131, Feb. 2022. doi: 10.3847/1538-4357/ac469f.

[6] C. Cardamone, K. Schawinski, M. Sarzi, S. P. Bamford, N. Bennert, C. M. Urry, C. Lintott, W. C. Keel, J. Parejko, R. C. Nichol, D. Thomas, D. Andreescu, P. Murray, M. J. Raddick, A. Slosar, A. Szalay, and J. Vandenberg. Galaxy Zoo Green Peas: discovery of a class of compact extremely star-forming galaxies. , 399(3):1191–1205, Nov. 2009. doi: 10.1111/j.1365-2966.2009.15383.x.

[7] M. K. Cavanagh, K. Bekki, and B. A. Groves. Morphological classification of galaxies with deep learning: comparing 3-way and 4-way CNNs. , 506(1):659–676, Sept. 2021. doi: 10.1093/mnras/stab1552.

[8] T.-Y. Cheng, M. Huertas-Company, C. J. Conselice, A. Aragón-Salamanca, B. E. Robertson, and N. Ramachandra. Beyond the hubble sequence - exploring galaxy morphology with unsupervised machine learning. , 503(3):4446–4465, May 2021. doi: 10.1093/mnras/stab734.

[9] S. P. Driver, S. Bellstedt, A. S. G. Robotham, I. K. Baldry, L. J. Davies, J. Liske, D. Obreschkow, E. N. Taylor, A. H. Wright, M. Alpaslan, S. P. Bamford, A. E. Bauer, J. Bland-Hawthorn, M. Bilicki, M. Bravo, S. Brough, S. Casura, M. E. Cluver, M. Colless, C. J. Conselice, S. M. Croom, J. de Jong, F. D'Eugenio, R. De Propris, B. Dogruel, M. J. Drinkwater, A. Dvornik, D. J. Farrow, C. S. Frenk, B. Giblin, A. W. Graham, M. W. Grootes, M. L. P. Gunawardhana, A. Hashemizadeh, B. Häußler, C. Heymans, H. Hildebrandt, B. W. Holwerda, A. M. Hopkins, T. H. Jarrett, D. Heath Jones, L. S. Kelvin, S. Koushan, K. Kuijken, M. A. Lara-López, R. Lange, Á. R. López-Sánchez, J. Loveday, S. Mahajan, M. Meyer, A. J. Moffett, N. R. Napolitano, P. Norberg, M. S. Owers, M. Radovich, M. Raouf, J. A. Peacock, S. Phillipps, K. A. Pimbblet, C. Popescu, K. Said, A. E. Sansom, M. Seibert, W. J. Sutherland, J. E. Thorne, R. J. Tuffs, R. Turner, A. van der Wel, E. van Kampen, and S. M. Wilkins. Galaxy And Mass Assembly (GAMA): Data Release 4 and the z < 0.1 total and z < 0.08 morphological galaxy stellar mass functions. , 513(1): 439–467, June 2022. doi: 10.1093/mnras/stac472.

[10] B. Henghes, C. Pettitt, J. Thiyagalingam, T. Hey, and O. Lahav. Benchmarking and scalability of machine-learning methods for photometric redshift estimation. , 505(4):4847–4856, Aug. 2021. doi: 10.1093/mnras/stab1513.

[11] B. D. Johnson, J. Leja, C. Conroy, and J. S. Speagle. Stellar Population Inference with Prospector. , 254 (2):22, June 2021. doi: 10.3847/1538-4365/abef67.

[12] D. P. Kingma and J. Ba. Adam: A Method for Stochastic Optimization. *arXiv e-prints*, art. arXiv:1412.6980, Dec. 2014. doi: 10.48550/arXiv.1412.6980.

[13] K. L. Masters, M. Mosleh, A. K. Romer, R. C. Nichol, S. P. Bamford, K. Schawinski, C. J. Lintott, D. Andreescu, H. C. Campbell, B. Crowcroft, I. Doyle, E. M. Edmondson, P. Murray, M. J. Raddick, A. Slosar, A. S. Szalay, and J. Vandenberg. Galaxy Zoo: passive red spirals. , 405(2):783–799, June 2010. doi: 10.1111/j.1365-2966.2010.16503.x.

[14] S. Ravanbakhsh, F. Lanusse, R. Mandelbaum, J. Schneider, and B. Poczos. Enabling Dark Energy Science with Deep Generative Models of Galaxy Images. *arXiv e-prints*, art. arXiv:1609.05796, Sept. 2016. doi: 10.48550/arXiv.1609.05796.

[15] S. Salim. Green Valley Galaxies. *Serbian Astronomical Journal*, 189:1–14, Dec. 2014. doi: 10.2298/SAJ1489001S.

[16] H. Torabi, S. L. Mirtaheri, and S. Greco. Practical autoencoder based anomaly detection by using vector reconstruction error. *Cybersecurity*, 6(1):1, 2023.

[17] B. Wang, J. Leja, V. A. Villar, and J. S. Speagle. SBI^{++}: Flexible, Ultra-fast Likelihood-free Inference Customized for Astronomical Applications. , 952(1):L10, July 2023. doi: 10.3847/2041-8213/ace361.

[18] F. Zou, W. N. Brandt, C.-T. Chen, J. Leja, Q. Ni, W. Yan, G. Yang, S. Zhu, B. Luo, K. Nyland, F. Vito, and Y. Xue. Spectral Energy Distributions in Three Deep-drilling Fields of the Vera C. Rubin Observatory Legacy Survey of Space and Time: Source Classification and Galaxy Properties. , 262(1):15, Sept. 2022. doi: 10.3847/1538-4365/ac7bdf.